Report on production of cement particles and characterization of steel and cement suspensions

Authors : Dr. Jerome ROSE (AMU), Slomberg Danielle (AMU-CEREGE), Auffan Mélanie (AMU-CEREGE), Payet Mickaël (IRSN), Gensdarmes François (IRSN), Mallard Véronique (CEA).

TRANSAT - Contract Number: 754586

Project officer: Project Officer: Angelgiorgio IORIZZO

Document title	Report on production of cement particles and characterization of steel and cement suspensions
Author(s)	Dr. Jerome ROSE, Slomberg Danielle (AMU-CEREGE), Auffan Mélanie (AMU-CEREGE), Payet Mickaël (IRSN), Gensdarmes François (IRSN), Mallard Véronique (CEA).
Number of pages	18
Document type	Deliverable
Work Package	WP03
Document number	D3.2
Issued by	AMU
Date of completion	2019-11-19 19:32:06
Dissemination level	Public

Summary

D3.2 is related to task 3.1 "Production and characterization of tritiated products" and more specifically Action 2 "Particles production" and Action 3 "Particles characterization". The production of cement particles was based on the methodology developed in action 1 by IRSN. The first tests permit to assess the particle production rate at 260 mg/min. This huge rate compared to steel particles (approximately 70 µg/min) induces adaptations on the set-up. The main issues are to isolate the particles with desired size and to manage airflow rate and sampling line according to filter clogging. The new design was carried out and the new set-up is operational. The characterisation of the stainless-steel particles focused both on particles generated by cutting devices as well as the commercial particles. The characterisation of the generated powder was detailed in deliverable 3-1. The physical-chemical stability of stainless-steel particles in aqueous media was tackled mainly via the characterisation of the particle size evolution using a combination of tools from light scattering, particle counters and UV-Vis spectroscopy. The initial average hydrodynamic diameter of steel particles varied from 6.3, 7.7 µm when concentration increased from 0.1 to 0.5 mg/l in ultrapure water. The initial size increased from 7.2 and 10.7µm for 0.1 mg/l and 0.5 mg/l in saline water. Based on the previous characterisation it was possible to set-up a robust preparation protocol for the stock suspension of SS316L particles requested for the future toxicological tests. In biological media, it was evidenced that surface dissolution after 7 days occurred for the stock suspension. Between 1.99 to 2.91 ±0.2 µg/l of Cr were released in saline and LHC9 medium. Nickel was also detected at slightly lower concentration. SS316L particles having been subjected to a hydrogenation treatment similar to that required for tritiation were also tested. Metal release kinetics of the pristine particles are not the same as for hydrogenated particles. It was thus decided that all subsequent experiments must be performed on hydrogenated SS316L particles to best represent the behaviour of the tritiated particles. The physical-chemical stability of cement particles was tested in aqueous media mainly to determine the pH buffer capacity of cement particles. The buffer capacity of the 2g/l cement particle suspension is high. More than 12 mmol of H+ are required to reach a stable pH value of 7.8-7.5.

Approval

Date	By
2019-11-20 09:43:50	Mrs. Veronique MALARD (CEA)
2019-11-20 09:54:59	Mr. Christian GRISOLIA (CEA)

DL. 3.2: Report on production of cement particles and characterization of steel and cement suspensions.

Deliverable:	D3.2
Work Package:	WP3
Due date of delivery:	According to DOA 28/02/2019
Document status:	Final
Submitted by:	Mallard Véronique (CEA)
Lead author:	Rose Jérôme (AMU-CEREGE)
Contributing authors	Slomberg Danielle (AMU-CEREGE), Auffan Mélanie (AMU-CEREGE), Payet Mickaël (IRSN), Gensdarmes François (IRSN), Mallard Véronique (CEA).

Document history

Version	Date	Who	Reason for change
0	01/02/2019	Rose Jérôme	First draft
1	01/03/2019		Cement characterisation added.
2	01/09/2019		Conclusion

Table of contents

Index of Tables

Table 4: cement alteration conditions. (The calculated surface area for parallelepipedic shape was (2x2x4 mm): Surface 1 grain = 40 mm2 = 0,4 cm2 => surface = 40 cm2/beaker) 15

Table of figures

Abbreviations

EC DG RTD	European Commission – Directorate General for Research and Innovation
DoA	Description of Action
ECCP	Electronic Collaborative Content Platform
ExCom	Executive Committee
GB	Governing Board
GB	Governing Board
PMO	Project Management Office
PQP	Project Quality Plan
PR	Periodic report
QA	Quality assurance
WP	Work package
WPL	Work package leader
SEM	Scanning Electron Microscope
XRD	X-ray Diffraction
HEPES	4-(2-hydroxyethyl)-1-piperazineethanesulfonic acid
MQ	Ultra-pure water
C-S-H	Calcium Silicate Hydrates (cement phase)
AFm	alumina, ferric oxide, monosulfate (cement phase)

Summary

DL3.2 is related to task 3.1 "Production and characterization of tritiated products" and more specifically Action 2 "Particles production" and Action 3 "Particles characterization".

The production of cement particles was based on the methodology developed in action 1 by IRSN. The first tests permit to assess the particle production rate at 260 mg/min. This huge rate compared to steel particles (approximately 70 µg/min) induces adaptations on the set-up. The main issues are to isolate the particles with desired size and to manage airflow rate and sampling line according to filter clogging. The new design was carried out and the new set-up is operational.

The characterisation of the stainless-steel particles focussed both on particles generated by cutting devices as well as the commercial particles. The characterisation of the generated powder was detailed in deliverable 3-1.

The physical-chemical stability of stainless-steel particles in aqueous media was tackled mainly via the characterisation of the particle size evolution using a combination of tools from light scattering, particle counters and UV-Vis spectroscopy. The initial average hydrodynamic diameter of steel particles varied from 6.3, 7.7 µm when concentration increased from 0.1 to 0.5 mg/l in ultrapure water. The initial size increased from 7.2 and 10.7µm for 0.1 mg/l and 0.5 mg/l in saline water. Based on the previous characterisation it was possible to set-up a robust preparation protocol for the stock suspension of SS316L particles requested for the future toxicological tests.

In biological media, it was evidenced that surface dissolution after 7 days occurred for the stock suspension. Between 1.99 to 2.91 ±0.2 µg/l of Cr were released in saline and LHC9 medium. Nickel was also detected at slightly lower concentration. SS316L particles having been subjected to a hydrogenation treatment similar to that required for tritiation were also tested. Metal release kinetics of the pristine particles are not the same as for hydrogenated particles. It was thus decided that all subsequent experiments must be performed on hydrogenated SS316L particles to best represent the behaviour of the tritiated particles.

The physical-chemical stability of cement particles was tested in aqueous media mainly to determine the pH buffer capacity of cement particles. The buffer capacity of the 2g/l cement particle suspension is high. More than 12 mmol of H+ are required to reach a stable pH value of 7.8-7.5.

1 Cement particles production

1.1 Cement setting

Anhydrous Portland cement (PC) was hydrated with ultra-pure water (UPW) at water/cement ratios (w/c) of 0.3, 0.4 and 0.5 to produce cement pastes with a range of initial porosity. Cement pastes were moulded in 20.5 (L) x 2(h) X 8.5 (l) cm plates. 300 grams of cement were used and samples were duplicated. Cement pastes were cured under water saturated atmosphere at room temperature for 28 days.
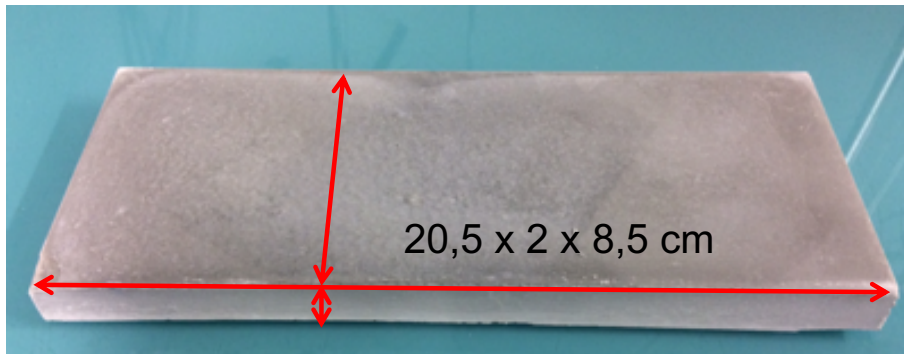
Figure 1: cement pastes after 28 days of setting

The following figure indicates that the hydration occurred with the formation of Calcium Silicate Hydrates (C-S-H) even if some anhydrous minerals (alite) still exist.
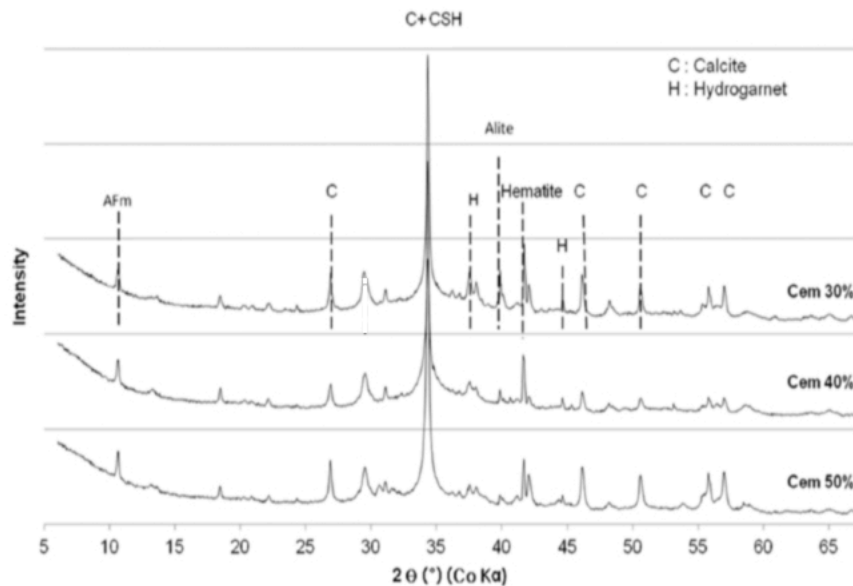
Figure 2: XRD analysis of hydrated cements

1.2 Cement particles production: first attempt

Cement particles were produced by using the device previously developed in the case of stainless-steel production (deliverable 3.1) in a confined environment (glove box) equipped with optical particle counters as illustrated in Figure 3. Cement samples were cut using Makita DGA506RTJ (18 V) with brushless motor delivering 8 500 rpm at the maximum (Figure 4-a). Diamond disks type *Standard for stone* from Bosch are used for cutting (Figure 4-b).
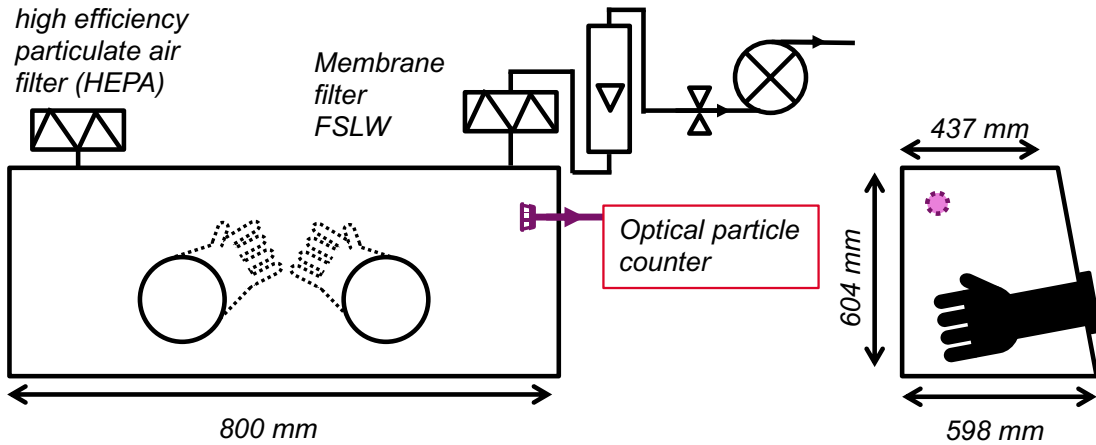
Figure 3: Particle production device.

Figure 4: Pictures of a) the *Makita DGA506RTJ* grinder and b) the diamond disk (Ø125 mm) used for the cutting of cement plates

Figure 5 illustrates the number of particles generated during the cutting of the cement plate width. Particle number exceeds 2×10^6, which corresponds to the detection limit of the optical particle counter, *Grimm 1.109* (OPC). However, the emission due to the disk grinder is measured at approximately 1.5×10^5 particles per litre for 2 minutes of continuous operation.
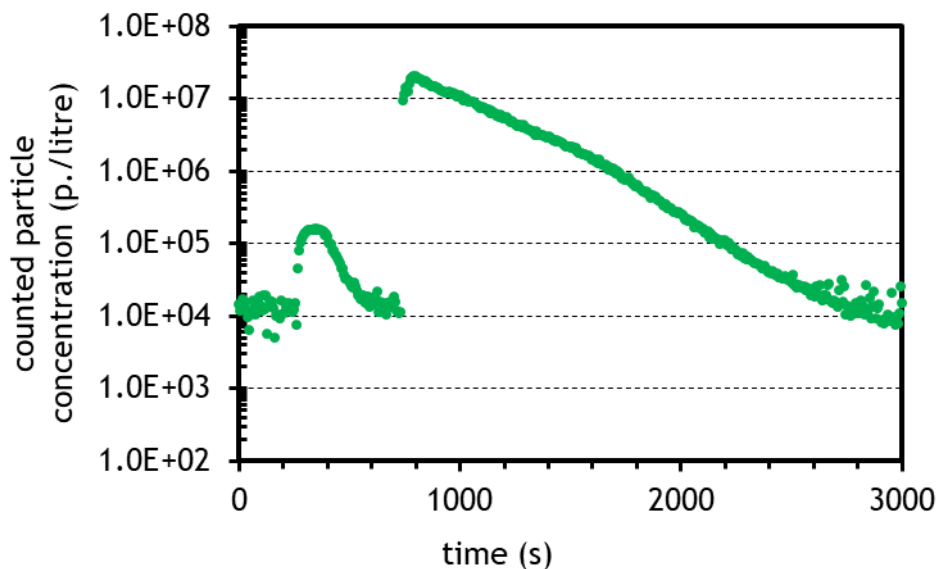
Figure 5: aerosol particles weight concentration and counted aerosol particles concentration produced during the cutting of cement.

The Figure 6 represents the particle concentration for three channels during the operation of the disk grinder without cutting. It shows that there is almost no particle emitted with a diameter above 1µm. Indeed, the concentration of emitted particles decreases with increasing particle diameter (from 0.25 to 1 µm of diameter). Similar results were obtained for the brushless reciprocating saw used for the steel particle production (deliverable 3.1).
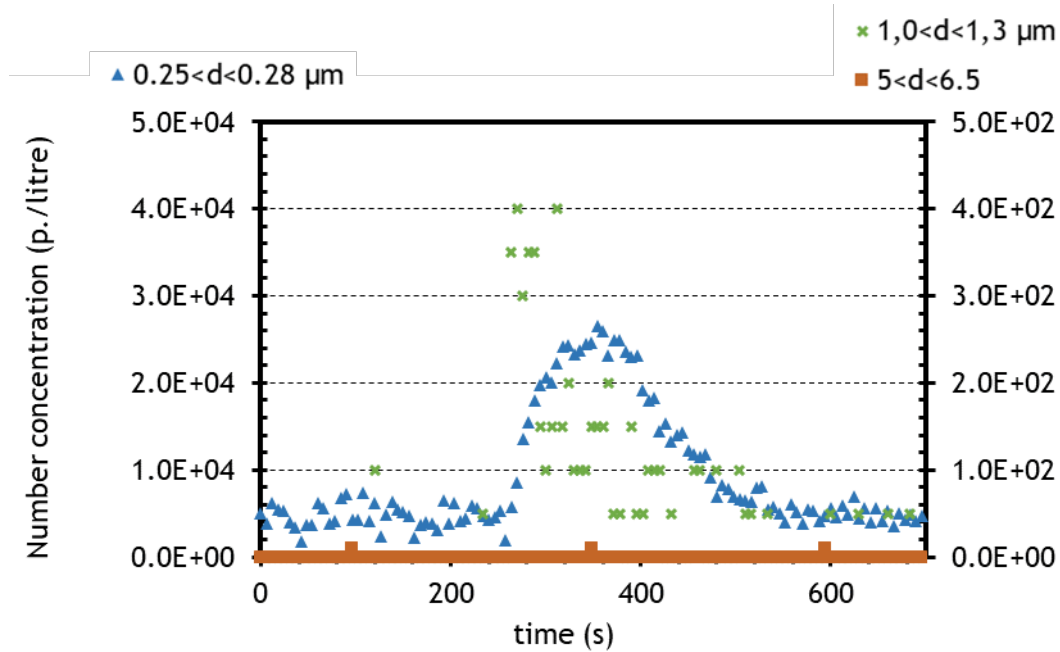
Figure 6: Evolution of the number concentration in the glove box during the disk grinder working without cutting.

The results obtained by the OPC during the cutting highlights the high emission rate of particles for three channels, diameters from 0.25 to 0.28 µm, from 1.0 to 1.3 µm and from 5 to 6.5 µm (Figure 7). The cutting starts at 740 s for 40 s. However, particles are detected during more than 1 000 s. The evolution of the number concentration in the range 0.25 to 0.28 µm reveals that the OPC have operated in oversaturation condition. Therefore, these data can not be used for the size distribution characterisation.
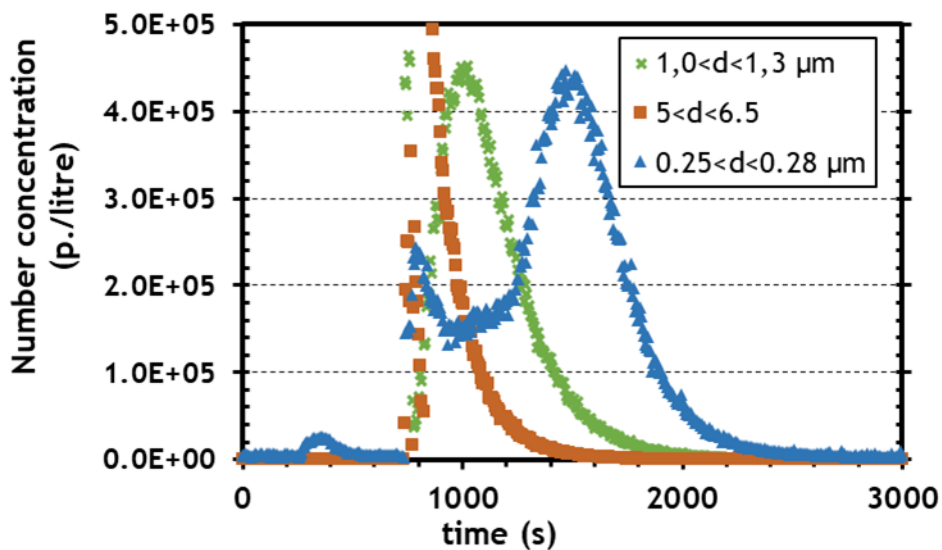
Figure 7: Evolution of the number concentration in the glove box during cutting phase for three channels (diameters from 0.25 to 0.28 µm, from 1.0 to 1.3 µm and from 5 to 6.5 µm)

The quantity of produced dust was extremely high and lead to a significant deposit on the membrane filter (FSLW type, Ø 47 mm). This induced a decrease of the airflow from 185 L/min to 80 L/min in the time of the cutting. The aerosol emission rate is assessed roughly at 260 mg/min (3 order of magnitude higher than the emission rate for the steel particle production).

The size distribution of the filter deposit is presented in the Figure 8. Further investigations will come using an Andesen impactor.
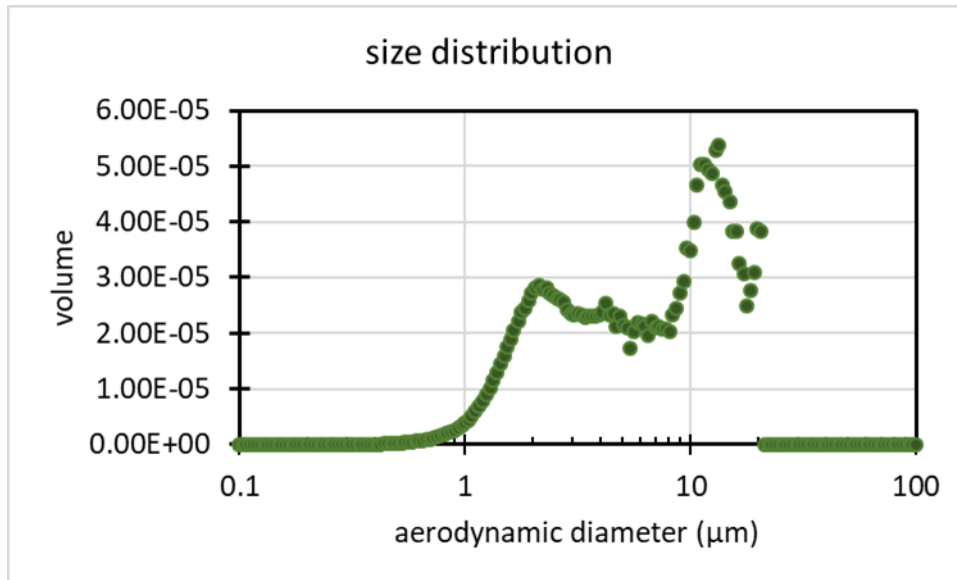
Figure 8: Size distribution of the cement particles generated during the cutting (analysis of the filter deposit)

The first attempt to produce particle cement with the available set-up leads to the following issues:
- the on-line particle monitor cannot operate with so high particle emission rate;
- the airflow decreases too fast because of the filter deposit during the cutting.

1.3 Cement particles production: set-up modification

The set-up modification aims to answer the mentioned issues:
- To limit the airflow decrease;
- To optimize the in-line size distribution of the aerosol emitted during the cutting.

In the same time, experimental constraints limit the adaptation of the extraction line. The nominal diameter is set to 40 mm. The modified set-up is presented on the Figure 9. An increase of the filter diameter from 47 mm to 140 mm would improve the collecting surface by a factor of 8. Consequently, the airflow decrease should be less important. Moreover, filter holder will be placed vertically to avoid deposition, as shown on the Figure 9. To measure the size distribution, an Andersen impactor samples the aerosol from the extraction line thanks to an isokinetic probe. Another kinetic probe could be linked to a cyclone cascade to select particles with an aerodynamic diameter below 10 µm.

A mass flow controller coupled with a sufficient pump (at least 240 L/min) is necessary to compensate the airflow decrease due to the deposit accumulation on the filter.

Q=200 L/min
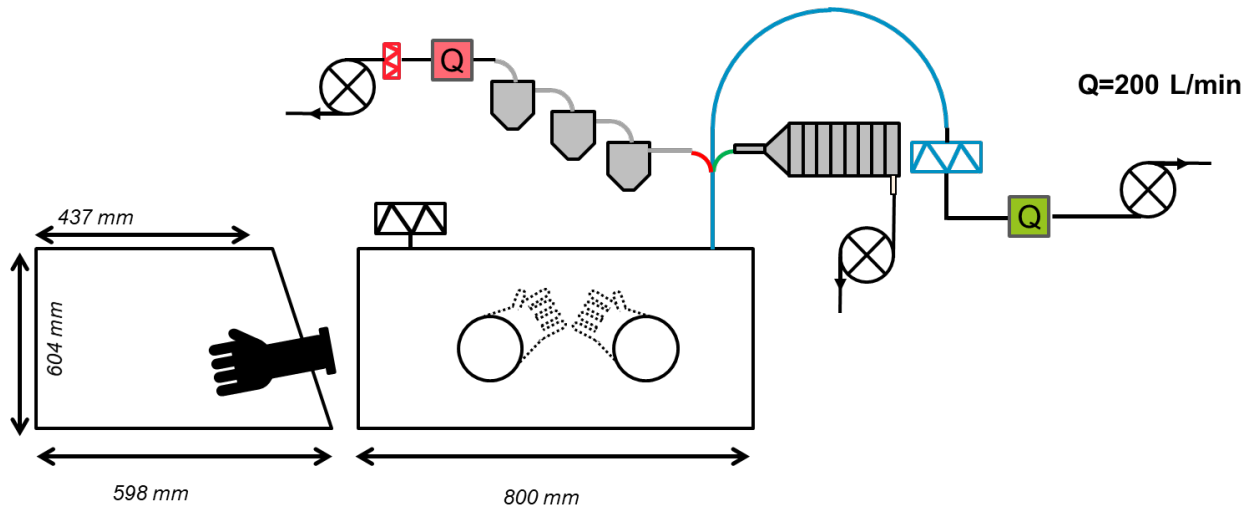
Figure 9: Scheme of the particle production set-up adapted for cement particles.

The extraction line and the isokinetic probes were specially designed using the aerosol calculation from Baron (2001) to sample the aerosol in a stabilised flow, and to avoid deposition and losses of particles in the bends and in the straight pipes (Figure 10). For the calculations, the used parameters are a temperature of 20°C, a pressure of 1.013×10^5 Pa, an airflow of 200 L/min for the extraction line, airflows of 28 L/min for the impactor and 8.5 for the cyclone. The collect efficiency was assessed for different particle sizes. Indeed, the efficiency decreases with an increasing aerodynamic diameter in the range of 0.5 to 20 µm. Consequently, the final design was optimised for particles with an aerodynamic diameter of 10 µm in agreement with the WP3 priorities. The Table 1 presents the global efficiency of each probe for these particles. 91% of the 10 µm-particles penetrating in the extraction line will be collected after the U-bend (so called "arch" bend).
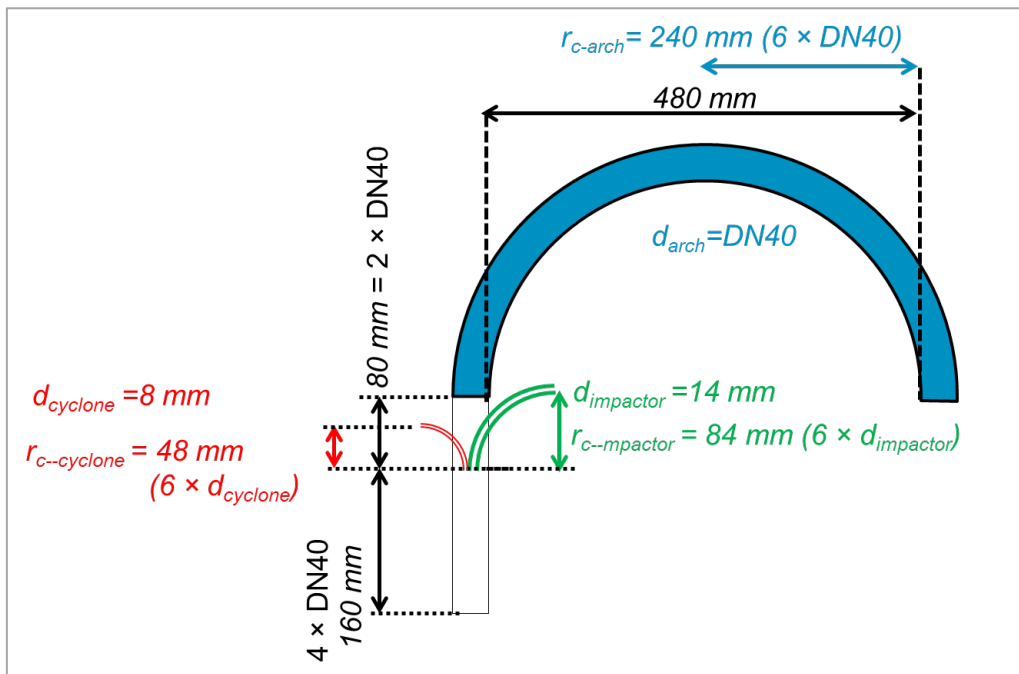
Figure 10: Probe design (d is the pipe diameter and r_c is the bend radius)

Table 1: Efficiency estimation for particles with a 10 μm aerodynamic diameter

	Impactor probe	Cyclone probe	Filter probe (extraction line)
Inlet efficiency	1.011	1.026	
Penetration fraction of the bend	0.89	0.82	0.91
Global efficiency	0.90	0.84	0.91

The set-up is now available.

2 Stainless steel particles characterisation

2.1 *Particles produced by cutting*

For the detailed characterisation of the stainless steel particles, reader must refer to the deliverable 3-1. Briefly, the produced particles using cutting devices were collected by deposition. Particle size ranged from 0.2 to 72 μm (Figure 11) as measured using optical particle counter.

Minimum = 0.22 μm
Maximum = 72.74 μm
Particles counted = 32 509
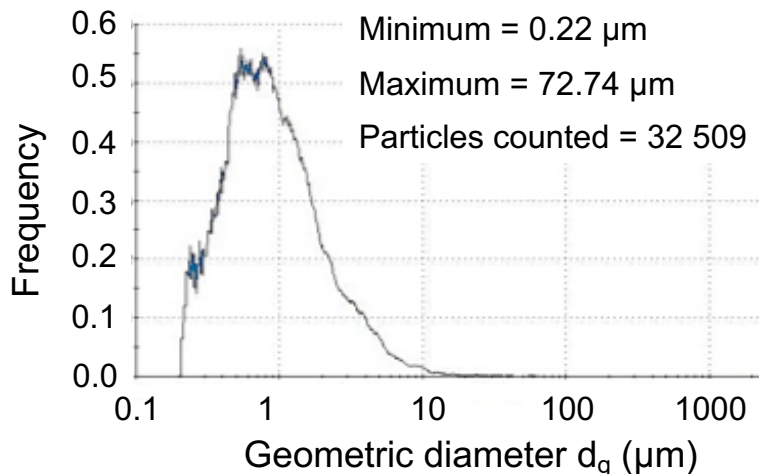
Figure 11: size distribution of the stainless-steel particles produced using the cutting device

The produced particles were modified by the cutting. A phase transformation occurred due to high mechanical stress which lead to the transformation of magnetic particles.

The morphology of the particles determined by SEM, mainly for the largest, was highly variable as shown on the following figure.
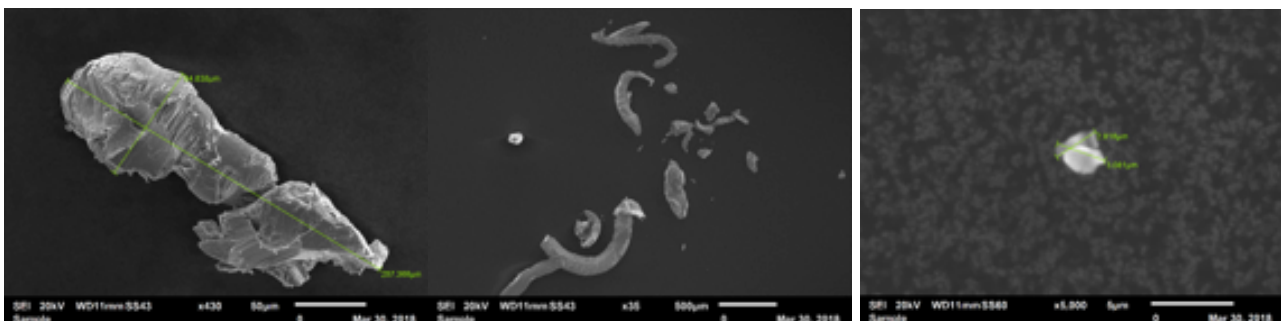
Figure 12: SEM images of some particles produced by the cutting device

2.2 Commercial particles (Goodfellow®)

The commercial SS317L powder are formed by the Fe/Cr/Ni alloy and also by Fe Austenite minerals as determined using X-ray diffraction.
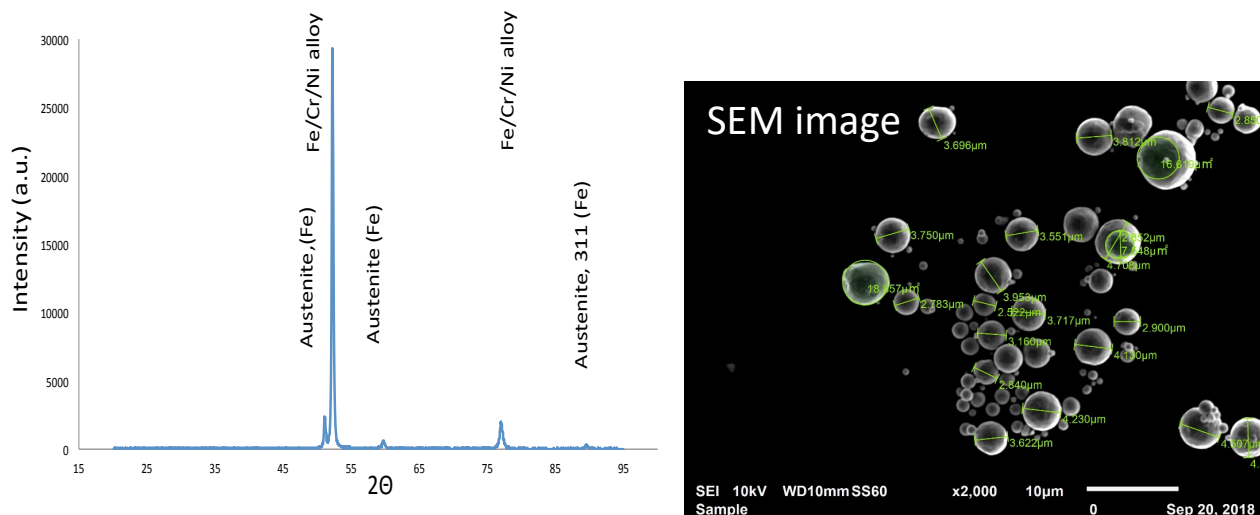
Figure 13: A) X-ray diffractogram and B) SEM image of the commercial SS316L powder

The powder is formed by poly-crystalline particles for which the sub-ordered domains extend from 47 to 108 nm as calculated with the Debye-Scherrer equation (Table 2).

Table 2: size of the ordered domains

Peak No.	Pos. 2θ	FWHM	Crystal size (nm)
1	51.08	0.195	88
2	52.21	0.260	108
3	59.67	0.325	56
4	76.92	0.227	97
5	89.41	0.455	47

The mean particle size claimed by the company was 3 µm and was almost confirmed by SEM analysis (Figure 13B).

2.3 Physical-chemical stability of commercial SS316L particles.

2.3.1 Colloidal stability in aqueous systems

The main objective of task 3.1 is to characterise and prepare particle suspensions to be tested for ecotoxicity and toxicity. The main issue with metallic particles in the 1-10 µm size range (inhaled particles that can reach alveolar regions) is related to their poor colloidal stability. The colloidal stability of the particle suspensions may be considered as one of the biggest challenges when (eco)-toxicity experiments are set-up. Indeed, the stability of the particles in the water column of the stock suspension will directly affect the accuracy of sampling and therefore the accuracy of the biological organism (or tissue) exposure.

UV-Vis spectroscopy was used to determine the settling velocity. The absorption coefficient was measured at 633 nm to determine the loss of mass within the water column. The settling velocity was determined in ultra-pure water at pH adjusted with HNO_3 from 5.6 to 8 as well as in saline

water (Saline solution = 0.9% NaCl, 1.25 mM $CaCl_2$, 10 mM HEPES) and as function of the initial concentration of SS316L particles.

Whatever the conditions more than 50% of the mas of the particles settled in 45 to 90 seconds (Figure 14A). The slowest mechanism occurred at the lowest pH and lowest initial concentrations.
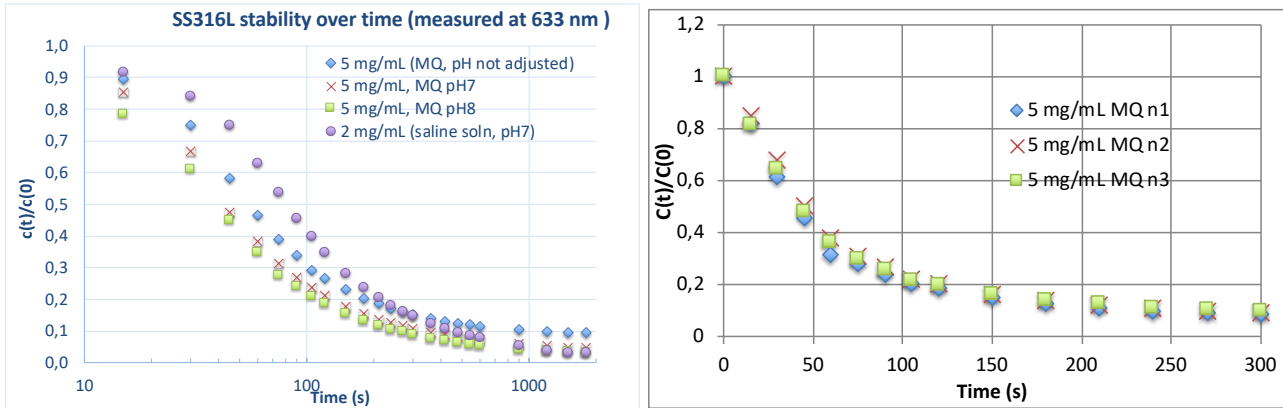
Figure 14: A) settling velocity of stainless-steel particles in various aqueous media (MQ: Ultra-pure water, Saline solution = 0.9% NaCl, 1.25 mM $CaCl_2$, 10 mM HEPES). B) repeatability of the settling experiment.

Even if the sedimentation of the particles occurred rapidly, the settling velocity is stable for a given condition. For instance, when repeated three times the settling velocity was found to be stable (SDT= 1,4%) (Figure 14B).

The sedimentation of the particles is not only related to the high density of the SS316L particle (d=7.87). Under steering at 150 rpm, aliquot from 5g/l stock suspension diluted and measured by laser diffraction (Malvern Mastersizer S), it was found that the steel particles can aggregate and therefore increase their settling velocity. As function of the initial concentration and aqueous medium the aggregation from t=0 to 5/10 minutes slightly increased particle and aggregate sizes from 6.6 µm up to 14.4/14.7 µm for the highest concentration whatever salinity (Figure 15).
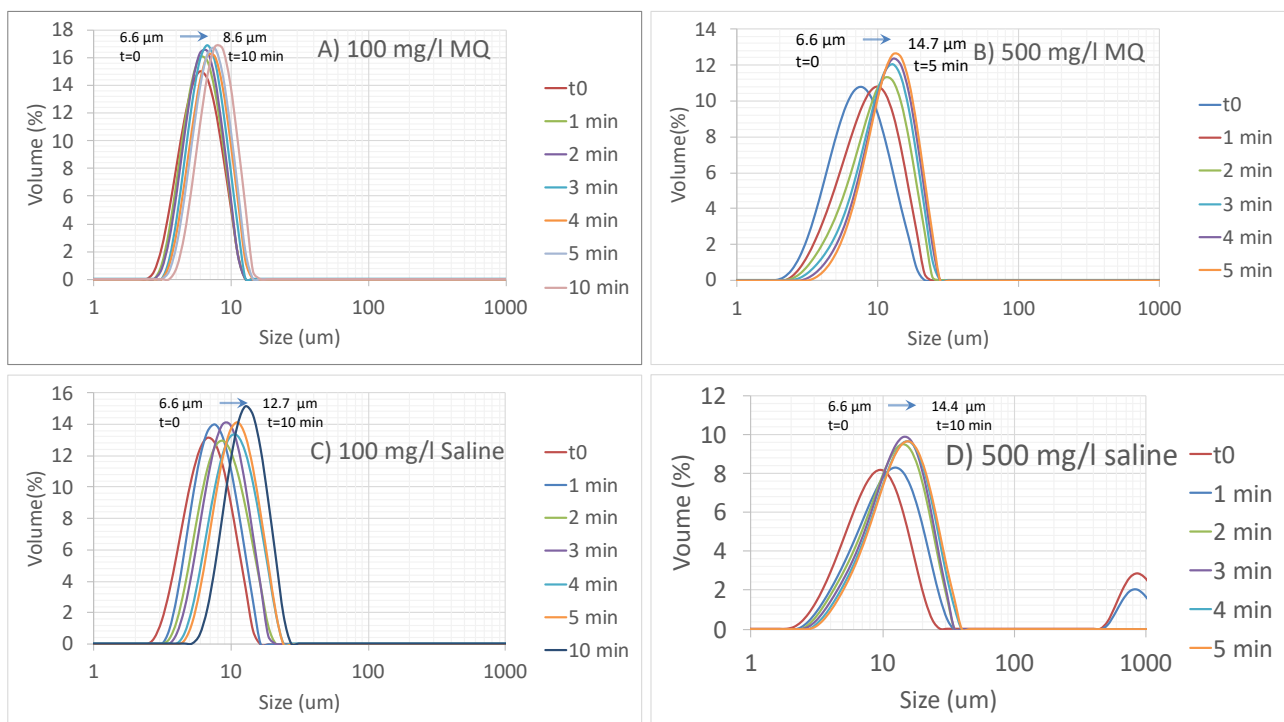

Figure 15: short term aggregation of SS316L particle in various media. (Saline solution = 0.9% NaCl, 1.25 mM CaCl2, 10 mM HEPES)

In the saline solution, very large aggregates were detected (few hundreds of μm)) at very short time but may have been des-aggregated due to steering.

The Occhio FC200S particle counter enabled to estimate the size and shape of SS316L particles in suspension. The result qualitatively confirmed the laser diffraction for which the signal is obtained as function of the volume fraction. Indeed, the particles size diameters at t=0 were centered on 6 μm and the signal of different stock suspensions remain reproducible. Particle images from the particle counter confirmed SEM analysis. Particles are more or less spherical, some aggregation was observed.
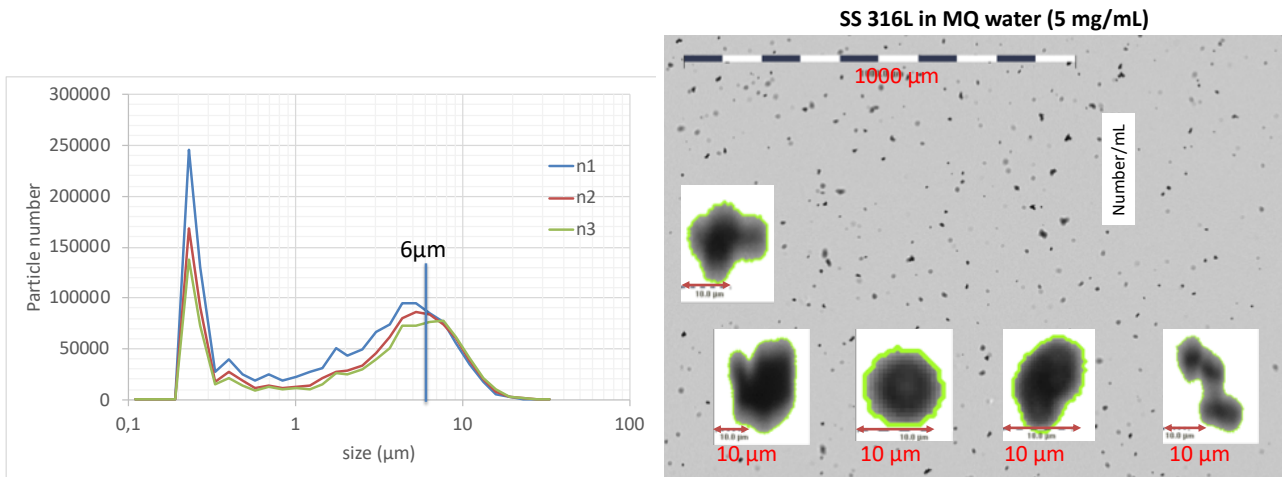

Figure 16: A) particle size distribution (number %) of 3 stock suspension replicates B) images of SS316L particles in solution

2.3.2   SS316L stock suspension preparation protocol

One important aspect of task 3.2 was to prepare stable stock suspension of SS316L particles to be used by toxicologists. The preparation of stock suspension requires recommendations to be followed in order to carry out toxicology experiments. For instance, the concentration should be higher than 2 g/l, the suspensions should be stable under optimized storage conditions.

As it was previously described, the commercial particles (3-4μm size dry state) are not stable while in aqueous medium. This clearly suggests that sampling aliquots from the stock suspension with constant concentration may be tricky. It was also found that the particles were sticking to the tube wall even only after one night and it was not possible to re-suspend them using vortex.

A first solution could have been to decrease the size of the SS316L particles to decrease the settling time and increase the ease of sampling. From the Stokes law[1] the time of settling in 1 cm water column was calculated and shown in the following table.

Table 3: particle settling time in 1 cm water column as function of size.

| Particle Size	Time
3 μm	74 s
1 μm	11 min
500 nm	45 min
100 nm	18.6 h

---

[1] Stokes law: Drag force $F_d = 6\pi\,\eta\,r\,v$ / Force of gravity $F_g = 4/3\,\pi r^3 (\rho_s - \rho_f) g$

F_d is the frictional force – known as Stokes' drag – acting on the interface between the fluid and the particle, η is the dynamic viscosity, r is the radius of the spherical particle, v is the flow velocity

To significantly increase the sampling time with a low sedimentation velocity of the SS316L particles, particle sizes below 500 nm might have been required. The various WP3 partners decided that decreasing the size of the particle below 500 nm may lead to affect the main objective of the project

It was therefore decided to develop suspension preparation and sampling protocols. The main objective was to enable all WP3 partners to prepare fresh stock suspension on a daily basis with a protocol as reproducible as possible. Previous results indicated that the sedimentation kinetics are reproducible for freshly prepared suspensions (Figure 14B). It was then crucial to determine whether it was possible to aliquot samples with a constant mass.

Three stock suspensions were prepared in which 3 aliquots were sampled. The concentration of the stock suspensions was 5 g/l. The stock suspensions were vortexed for 15 seconds. 0.5 ml of aliquot were samples with a predicted mass of SS316L particles of 2.5 mg. The pipet tips were changed each time. The results indicated that the Inter-sample variability and variability between samples remained below 5% (Figure 17).

	n1	n2	n3
Aliquot 1	2.6 mg	2.6 mg	2.7 mg
Aliquot 2	2.5 mg	2.7 mg	2.4 mg
Aliquot 3	2.5 mg	2.8 mg	2.2 mg
	2.5 ± 0.1 mg	2.7 ± 0.1 mg	2.4 ± 0.2 mg
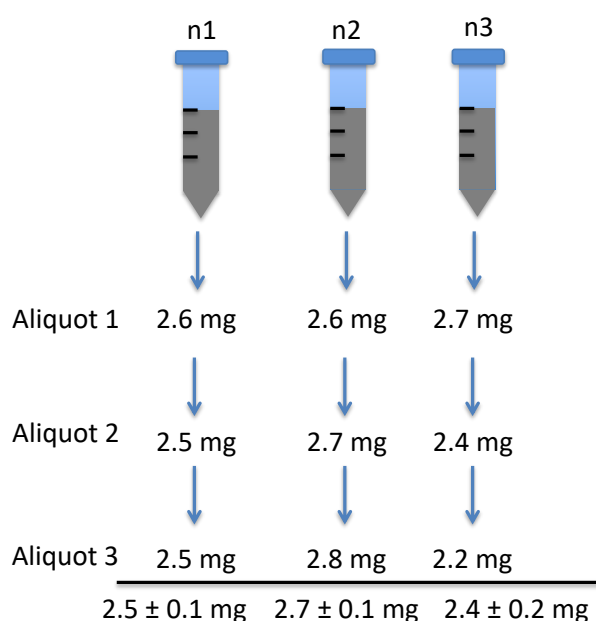
Proposed protocols for stainless-steel stock suspension preparation and sampling prior to biological tests

1. **Weigh SS 316L powder** in plastic centrifuge tube
2. **Add media** to get desired concentration
3. **Disperse until homogenous** using vortex ~ 15 sec, 2500/min
4. Pipet aliquot **immediately** from centre of suspension
5. **Change pipet tip** in between every aliquot to avoid particles sticking between samples

Figure 17: A) reproducibility of the preparation and sampling protocol and B) details of the proposed protocol.

The proposed protocol (Figure 17B) was introduced and accepted by WP3 partners.

2.3.3 SS316L digestion protocol

Another important task in characterizing the SS316L particles was to confirm their elemental composition and decide on a digestion protocol for the solid particles that could be used by all WP3 partners. The digestion parameters varied included the solid-to-liquid ratio (i.e., 50, 10, or 5 mg in 6.5 mL acid), the temperature (ambient or 200 °C), and the presence or absence of hydrofluoric acid (HF). Digested SS316L solutions were then analyzed for Fe, Cr, Ni, and Mo concentrations using inductively coupled plasma−atomic emission spectroscopy (ICP-AES).

The SS316L elemental composition given by the manufacturer was confirmed to be 68.8 % Fe, 17% Cr, 10% Ni, and 2% Mo. Based on the percent recoveries obtained after varying each parameter, we determined that the tested solid-to-liquid ratios, temperatures, and presence/absence of HF had no significant effect on SS316L digestion. Therefore, it was decided that all WP3 partners will digest 50 mg SS316L particles in an acid mixture (3 mL HCl, 1 mL HNO_3) at ambient temperature for 48 h to ensure safety and ease of manipulation. This digestion protocol

resulted in elemental recoveries of 94, 99, 97, and 111 % for Fe, Cr, Ni, and Mo, with an error of ~5% for all digestions.

2.3.4 SS316L chemical stability in biological media

The SS316L chemical stability in biological media was tested to evaluate the possibility of corrosion/dissolution during toxicology experiments. A stock SS316L suspension was prepared in MQ as described in section *2.3.2*. The stock SS316L suspension was then used to prepare test suspensions in saline water (0.9% NaCl, 1.25 mM $CaCl_2$, 10 mM HEPES) and the biological medium, LHC-9, at 0.1 g/l. The SS316L chemical stability SS316L was first evaluated after 1 day, 3 days, and 7 days at 37 °C. Samples were either maintained under static conditions, or they were mixed by roller agitation to represent a worst-case release scenario. At the end of the exposition, the samples were centrifuged (2675 *g*, 10 min) to separate the particles from the supernatant. The supernatant was recovered using a pipet and analyzed for Fe, Cr, and Ni concentrations using inductively coupled plasma–mass spectrometry (ICP-MS).

Preliminary results suggested that particle release of Fe could not be quantified due to a high and variable environmental background. However, Cr and Ni were detected above the background at µg/L concentrations. The type of agitation (i.e., static versus roller) had minimal impact on the chemical stability of the SS316L particles in either the saline or LHC-9 solutions, even after 7 days (Table 4). Subsequent stability tests were thus performed under static conditions, as no difference in stability was observed with agitation.

Table 4. Metal release from SS316L particles after 7 days under varied agitation conditions.

	Cr (µg/L)		Ni (µg/L)	
	Static	Roller	Static	Roller
saline water	2.91 ± 0.23	2.67 ± 0.27	1.23 ± 0.33	0.97 ± 0.19
LHC-9	1.99 ± 0.16	2.33 ± 0.04	1.52 ± 0.22	1.82 ± 0.53

Having defined the protocol for the SS316L chemical stability test, it was also aimed to compare metal release from the pristine (i.e., as-purchased) SS316L particles to SS316L particles having been subjected to a hydrogenation treatment similar to that required for tritiation. Using the same procedure described above, the sample supernatants were analyzed for Cr and Ni release at t0 and 15 min, 3 h, 6 h, 1 day, 3 days, and 7 days after static aging 37 °C.

As shown in Figure 18 at t0, some immediate Cr and Ni release was observed from the surface of both the pristine and hydrogenated SS316L regardless of the test solution. This also revealed that the metal release kinetics of the pristine particles are not the same as for hydrogenated particles. It was thus decided that all subsequent experiments must be performed on hydrogenated SS316L particles to best represent the behavior of the tritiated particles. Overall for the hydrogenated particles, there was ~0.004 % Cr release after 7 days in both the saline and LHC-9 medium. However, there was no significant dissolution of Ni from hydrogenated SS316L.
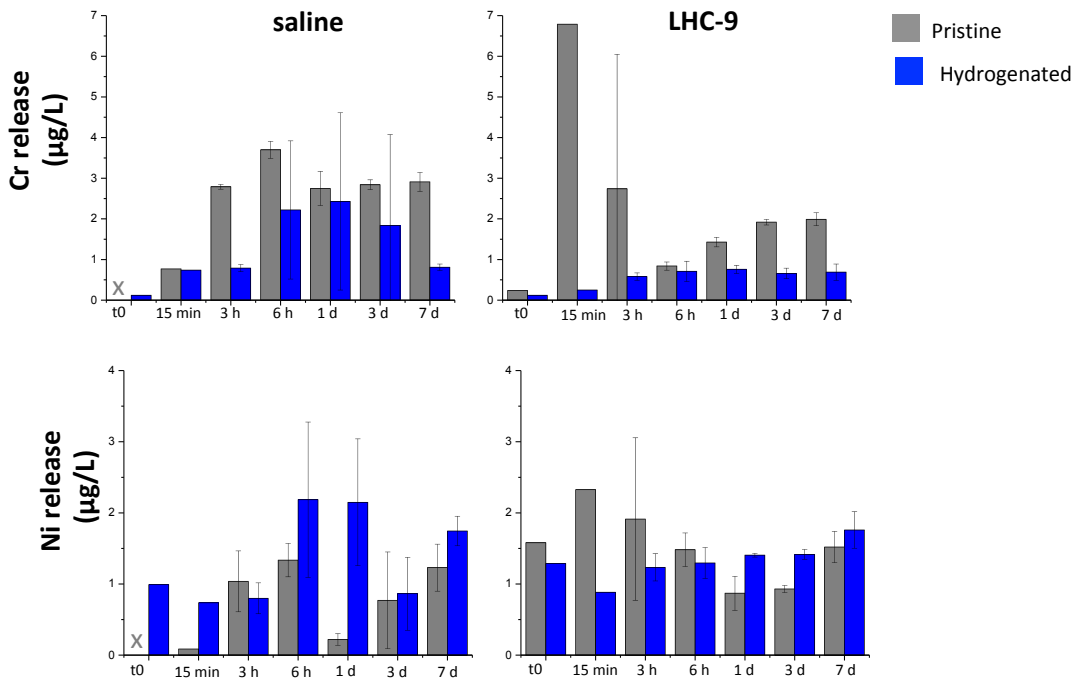
Figure 18. Time-dependent metal release from pristine (gray) and hydrogenated (blue) SS316L particles in biological media.

3   Cement particles characterisation

Even if the production of 1-10 µm cement particles was delayed, the characterisation of cement was launched.

A first set of characterisation experiment was performed on 2-4 mm cement particle size, easy to screen and separate.

3.1   2-4 mm cement particles suspension stability.

10 samples were prepared using at 3 fixed initial pHs (8, 9, 10). The parameters are summarized in the following table.

Table 4: cement alteration conditions. (The calculated surface area for parallelepipedic shape was (2x2x4 mm): Surface 1 grain = 40 mm2 = 0,4 cm2 => surface = 40 cm2/beaker)

Cement 2-4 mm

N° beaker	1	2	3	4	5	6	7	8	9	10
S (g) cement	2,061	2,034	2,018	2,051	2,095	2	2,079	2,041	2,027	2,09
Number of grains	79	97		95		82		128		96
L (ml) UPW	206	203,2	201,8	205,1	209,5	200,1	207,9	204,1	202,7	209
W/C	100,0	99,9	100,0	100,0	100,0	100,1	100,0	100,0	100,0	100,0

The chemical stability of the particles in a 2g/l suspension was tested over 150 hours. Due to the large size of the particles, the beakers were stirred using a shaking table.

Figure 19: cement suspension stirring device

The pH and the conductivity of the samples were scanned (Figure 20).
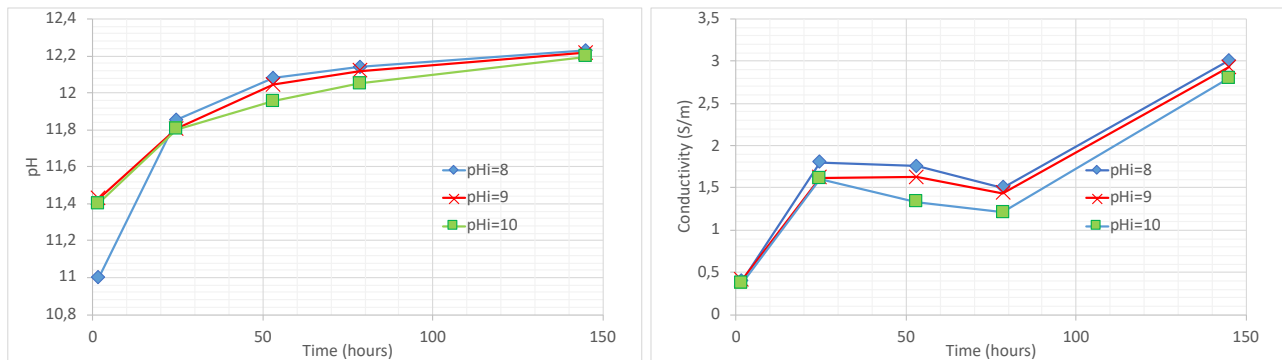
Figure 20: A) pH and B) conductivity evolution of the stirred suspensions with 3 initial pH (pHi).

Whatever the initial pH, the pH reached almost the same value after 24 hours and reached a plateau after 145 hours with a pH of 12.2/12.3. The evolution with time of the conductivity followed a different trend. Whatever the initial pH, the conductivity of the 3 systems reached the same value after 1.5 hours. The conductivity of the three systems increased up to 1.6-1.8 S/m at t=24h. Then a slight decrease occurred from t=24 hours to t=78 hours, with a final increase up to 145 hours. The final values ranged from 2.8 to 3.01 S/m.

The cement particles were altered as illustrated by the X-ray computed tomography images (Figure 21). The corroded layer reached 120 to 150 µm as illustrated on one altered grain. Such range of corrosion would suggest that for particle size in the 1-10 µm range, the corrosion would represent a strong effect since the particle would be altered from the surface to the core.
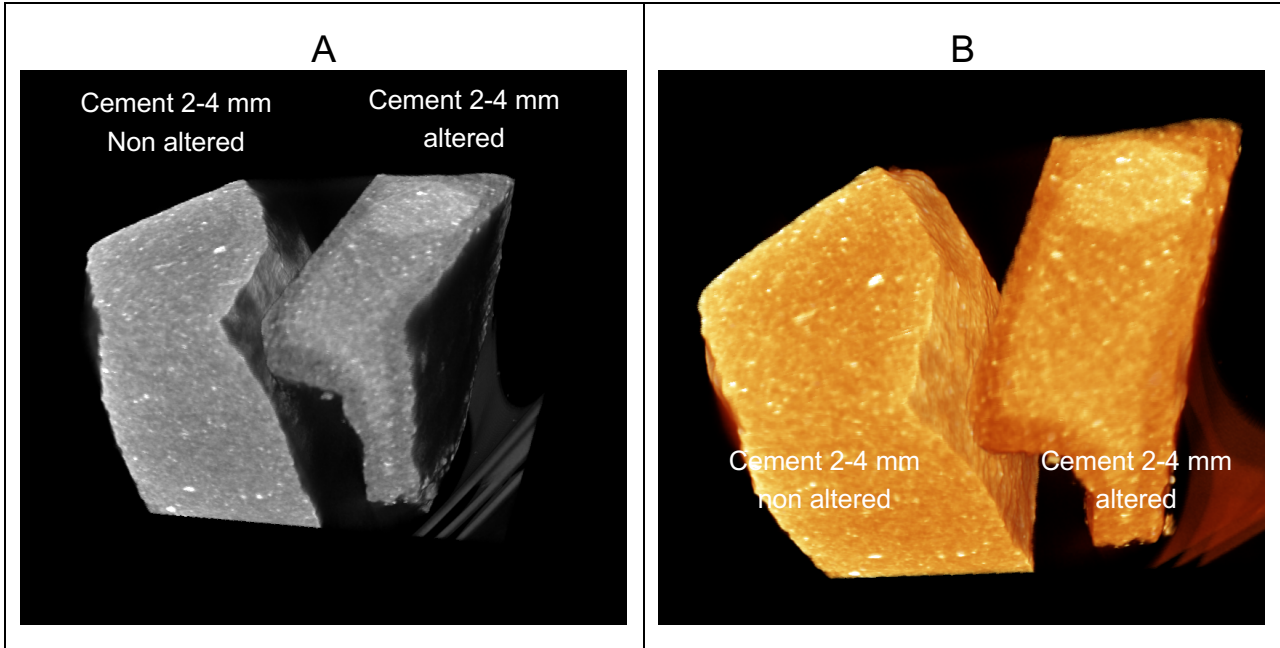
Figure 21: X-ray 3D images of two cement grains before and after corrosion during the stability experiment test. The grey zone (A) converted to dark orange (B) at the surface of the altered grain represent the corroded layer (120 to 150 μm)

The previous experiment revealed the high pH buffer capacity of cement suspensions with a concentration of 2 g/l which represent the target value for stock suspension preparation.

Suspensions with such high pH can not be used as stock suspension. Indeed, it would create a strong chemical stress leading to very high toxic effects. The role of particles would not be evidenced due to pH artefacts.

The buffer capacity of the cement suspensions at 2 g / l was then tested using titration experiments. The aim was to determine the number of moles of H+ to be added to reach a stable pH of 7.8 (≈biological pH).
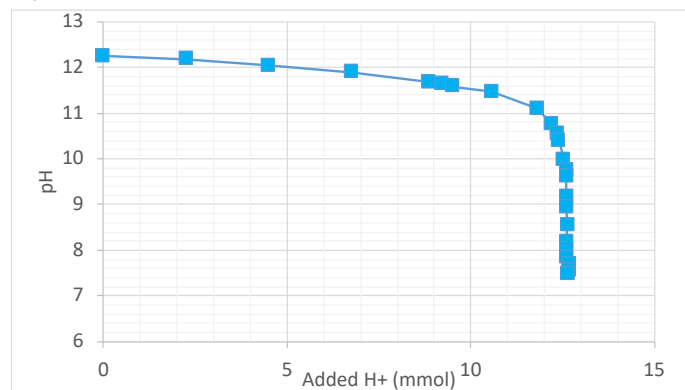

Figure 22: titration curve of the 2g/l cement suspensions.

The buffer capacity of the 2g/l cement particle suspension is high. More than 12 mmol of H+ are required to reach a stable pH value of 7.8-7.5. At the end of the titration experiment most of the cement particles dissolved, even if some colloids remained in suspension.

4 Conclusions

The present set-up for particle production permits to generate cement particles but needs modifications to characterise appropriately the aerosol. The aerosol production rate is estimated at 260 mg/L and the size distribution is in the range of 0.8 to 15 µm. A specific design of the sample probes has been studied to optimise the particle collection and characterisation. The modifications were validated and permit to collect efficiently (91%) particles below 10 µm of aerodynamic diameter.

The physical-chemical stability of stainless-steel particles in aqueous media was tackled mainly via the characterisation of the particle size evolution using a combination of tools from light scattering, particle counters and UV-Vis spectroscopy. The initial average hydrodynamic diameter of steel particles varied from 6.3, 7.7 µm when concentration increased from 0.1 to 0.5 mg/l in ultrapure water. The initial size increased from 7.2 and 10.7µm for 0.1 mg/l and 0.5 mg/l in saline water.

The characterisation of the stainless-steel particle stability in aqueous media enabled to elaborate a dispersion protocol which is essential to run toxicological tests. It is almost impossible to avoid SS particle settling. The standardized protocol proposes an alternative to prepare fresh stock suspensions with repeatable physical-chemical properties.

In biological media, it was evidenced that surface dissolution after 7 days occurred for the stock suspension. Between 1.99 to 2.91 ±0.2 µg/l of Cr were released in saline and LHC9 medium. Nickel was also detected at slightly lower concentration. SS316L particles having been subjected to a hydrogenation treatment similar to that required for tritiation were also tested. Metal release kinetics of the pristine particles are not the same as for hydrogenated particles. It was thus decided that all subsequent experiments must be performed on hydrogenated SS316L particles to best represent the behaviour of the tritiated particles.

In the case of cement, the dissolution of particles will lead to strong increase of pH and will strongly affect toxicological results. The buffer capacity of the 2g/l cement particle suspension is high. More than 12 mmol of H+ are required to reach a stable pH value of 7.8-7.5. Pre-maturation protocol that will decrease the pH buffer capacity of cement particles, will be adopted for the toxicological tests.